Experimental Investigation of Toluene + H → Benzyl + H_2 at High Temperatures

Matthew A. Oehlschlaeger*

Department of Mechanical, Aerospace, and Nuclear Engineering, Rensselaer Polytechnic Institute, Troy, New York 12180-3590

David F. Davidson and Ronald K. Hanson

Department of Mechanical Engineering, Stanford University, Stanford, California 94305-3032

Received: April 26, 2006; In Final Form: June 22, 2006

The reaction of toluene with hydrogen atoms yielding benzyl and molecular hydrogen, $C_6H_5CH_3 + H \rightarrow C_6H_5CH_2 + H_2$, was investigated using UV laser absorption of benzyl radicals at 266 nm in shock tube experiments. Test gas mixtures of toluene and ethyl iodide, an H-atom source, diluted in argon were heated in reflected shock waves to temperatures ranging from 1256 to 1667 K at total pressures around 1.7 bar. Measurement of laser absorption at 266 nm due to benzyl radicals allowed determination of the rate coefficient of the title reaction, reaction 1. A two-parameter best-fit Arrhenius expression for the rate determinations over the temperature range of these experiments is given by $k_1(T) = 1.33 \times 10^{15} \exp(-14880\ [\text{cal/mol}]/RT)$ $[\text{cm}^3\ \text{mol}^{-1}\ \text{s}^{-1}]$. With the use of both the high-temperature shock tube measurements reported here and the rate coefficient determination of Ellis et al. (Ellis, C.; Scott, M. S.; Walker, R. W. *Combust. Flame* **2003**, *132*, 291) at 773 K the best-fit rate coefficient for reaction 1 can be described using a three-parameter Arrhenius expression by $k_1(T) = 6.47T^{3.98} \exp(-3384\ [\text{cal/mol}]/RT)$ $[\text{cm}^3\ \text{mol}^{-1}\ \text{s}^{-1}]$.

Introduction

The reaction of toluene with H-atoms producing benzyl radicals and molecular hydrogen

$$C_6H_5CH_3 + H \rightarrow C_6H_5CH_2 + H_2 \qquad (1)$$

is an important elementary reaction in the toluene pyrolysis and oxidation reaction systems. Reaction 1 retards ignition during toluene oxidation by removing an H-atom that otherwise would lead to chain branching via reaction with O_2. Reaction 1 also produces a resonantly stable benzyl radical which reacts very slowly with molecular oxygen[1,2] and is generally only further oxidized by reaction with radicals. Detailed kinetic modeling by Pitz et al.,[3] Bounaceur et al.,[4] and Dagaut et al.[5] shows that experimental oxidation targets such as shock tube ignition delay, shock tube intermediate hydroxyl (OH) concentrations, flow reactor carbon monoxide (CO) yields, and jet-stirred reactor toluene conversion data all have large sensitivity for the rate coefficient of reaction 1, k_1. Therefore, accurate knowledge of this rate coefficient is needed for the improvement of future models developed for toluene combustion.

Previous high-temperature measurements for the reaction of toluene with H-atoms have been carried out using a variety of techniques. Rao and Skinner[6,7] investigated reaction 1 using time-resolved D-atom and H-atom atomic resonance absorption spectroscopy (ARAS) in shock-heated gases at temperatures ranging from 1200 to 1730 K with mixtures of two deuterated toluene species ($C_6D_5CD_3$ and $C_6H_5CD_3$) and H-atom sources. Rao and Skinner related their results to the reaction of toluene with H-atoms using corrections for isotopic effects. Braun-Unkhoff et al.[8] measured H-atoms via ARAS in shock tube toluene decomposition experiments from 1380 to 1700 K and provided an indirect estimate of the reaction 1 rate coefficient. Robaugh and Tsang[9] carried out single-pulse shock tube experiments using gas chromatograph measurements of quenched product gas concentrations to determine k_1 in the temperature range of 950−1100 K. Time-resolved UV lamp absorption of benzyl radicals was employed by Hippler et al.[10] to determine k_1 in the temperature range from 1300 to 1700 K in shock-heated gases. Most recently, Ellis et al.[1] determined the rate coefficient for reaction 1 at 773 K by adding small concentrations of toluene to $H_2/O_2/N_2$ mixtures in a heated cylindrical static reactor and measuring product gas composition using gas chromatography. These previous experimental studies produced rate coefficient determinations for reaction 1 that differ by about a factor of 2; additionally, the most recent International Union of Pure and Applied Chemistry (IUPAC) evaluation (Baulch et al.[11]) recommends a rate coefficient with an estimated uncertainty of a factor of 2. In light of the span in the previous experimental rate coefficient measurements, the estimated uncertainty in the rate coefficient recommendations, and the importance of this reaction in modeling toluene oxidation, we have performed new experimental measurements of k_1 with reduced scatter and uncertainty.

Here we present measurements of k_1 using UV laser absorption of benzyl in shock-heated mixtures of toluene and ethyl iodide, an H-atom precursor, diluted in argon. Spectrally intense laser radiation provides higher signal-to-noise (approximately a factor of 10) than previous lamp measurements[10] allowing improved fitting of kinetic calculations to the experimentally measured absorbance for the purpose of rate coefficient determination. Additionally, the increased signal-to-noise allows for experiments to be performed using lower initial concentrations of H-atom precursor, reducing the dependence of the determined rate coefficient on secondary chemistry.

* Corresponding author. Phone: 518-276-8115. Fax: 518-276-6025. E-mail: oehlsm@rpi.edu.

10.1021/jp062567t CCC: $33.50
Published on Web 07/22/2006

Experimental Section

The experiments described here were performed behind reflected shock waves in a pressure-driven stainless steel shock tube facility previously described in Oehlschlaeger et al.[12−14] Reflected shock conditions ranged from 1256 to 1667 K at total pressures around 1.7 bar. Test gas mixtures were made manometrically using ethyl iodide (99.5% purity), toluene (99% purity), and argon (99.999% purity) in a high-purity turbopumped heated stainless steel mixing tank with an internal stirring system. A high-accuracy Baratron capacitance manometer was used to measure the partial pressure of the individual species contained in the mixtures, and the tank was heated to 60 °C to avoid wall absorption of ethyl iodide. The ethyl iodide and toluene were cycled through several freeze−pump−thaw cycles prior to introduction into the mixing tank to avoid impurities from high-volatility species. Two different test gas mixtures were used: 30 ppm ethyl iodide/506 ppm toluene/argon and 50 ppm ethyl iodide/513 ppm toluene/argon. Mixtures were allowed to mix overnight prior to shock wave experiments to allow for complete mixing. Additionally, the kinetic results obtained in these experiments were repeatable with no observed influence from variations in the initial ethyl iodide concentration, the mixing time, or the mixing tank temperature providing confidence in the initial ethyl iodide concentrations in the test gas mixtures determined manometrically.

Benzyl radicals were detected using laser absorption at 266 nm, a detection technique that has been previously developed[13] and applied in kinetic studies of benzyl radical decomposition[13] and toluene decomposition.[14] Continuous wave laser radiation was generated at 266 nm (1.5 mW) by the single pass of a focused, 5 W, 532 nm laser beam (frequency-doubled Nd:YVO_4) through an angle-tuned beta barium borate (β-BaB_2O_4, BBO) crystal. After generation, the harmonic (266 nm) was separated from the fundamental (532 nm) in a Pellin−Broca prism. The 266 nm laser beam was split into two components: one, ∼1 mm in diameter, passing through the shock tube as a diagnostic beam (I), and one detected prior to absorption as a reference (I_0). Absorption measurements were made across the shock tube diameter at a location 2 cm from the endwall. The shock-heated gases were accessed through 0.75 in. diameter flat wedged windows made of UV fused silica flush mounted to the inner radius of the shock tube. The intensities of the reference and diagnostic beams were measured using amplified silicon photodiodes (Hamamatsu S1722-02, rise time < 0.5 μs, 4.1 mm diameter) and recorded on a digital oscilloscope.

The benzyl absorption cross-section at 266 nm has been previously measured by shock heating mixtures of benzyl iodide diluted in argon to produce known, instantaneous, postshock benzyl yields.[13] In addition, the absorption cross-sections of toluene and of the benzyl decomposition product (a C_7H_6 molecule of unknown structure) have been determined previously.[13,14] The 266 nm absorption cross-sections for benzyl ($C_6H_5CH_2$), benzyl fragments (C_7H_6), and toluene ($C_6H_5CH_3$) used in this study are as follows: $\sigma_{C_6H_5CH_2}(266\text{ nm}) = 1.9\ (\pm 0.2) \times 10^{-17}$ cm^2 molecule^{-1}, $\sigma_{C_7H_6}(266\text{ nm}) = 3.4\ (\pm 0.5) \times 10^{-18}$ cm^2 molecule^{-1}, and $\sigma_{C_6H_5CH_3}(266\text{ nm}) = 5.9\ (\pm 0.6) \times 10^{-19}$ cm^2 molecule^{-1}. The 266 nm absorption cross-sections of these species showed no discernible temperature dependence across the experimental range of the previous benzyl iodide and toluene experiments[13,14] (1400−1800 K), and in other unpublished experiments by our group they have shown no temperature dependence down to 1100 K. In addition, ethyl iodide and ethylene (the product of ethyl iodide decomposition) absorb at 266 nm at high temperatures. The 266 nm absorption cross sections of ethyl iodide and ethylene were quantified prior to performing the experiments described here by shock heating mixtures of ethyl iodide and ethylene diluted in argon. The resulting cross-sections are $\sigma_{C_2H_5I}(266\text{ nm}) = 8\ (\pm 2) \times 10^{-19}$ cm^2 molecule^{-1} and $\sigma_{C_2H_4}(266\text{ nm}) = 2.0\ (\pm 0.4) \times 10^{-19}$ cm^2 molecule^{-1} again with no discernible temperature dependence. However, absorption due to ethyl iodide and ethylene is minimal in the experiments described here due to the low concentrations of ethyl iodide relative to that of toluene present in the test gas mixtures. Absorption due to other interfering species (CH_3, C_6H_5, C_6H_6, C_6H_4, and $C_6H_5CH_2CH_2C_6H_5$) was considered but found to be negligible due to the smaller absorption cross-sections at 266 nm of these species and the small concentrations of these species present during these experiments. However, uncertainty in the interfering absorption was accounted for in the estimate of uncertainty in the resulting rate coefficient.

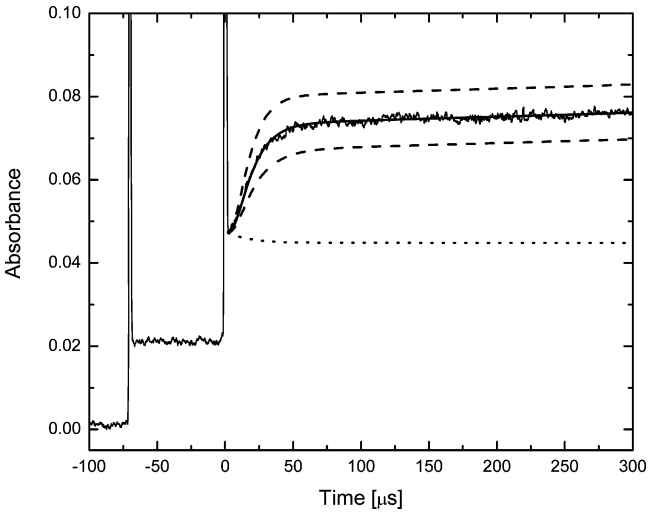

Figure 1. Example 266 nm absorbance. Reflected shock conditions: 1313 K, 1.87 bar, 30 ppm ethyl iodide/506 ppm toluene/argon. Solid line, fit to data by adjusting reaction 1 rate coefficient, k_1; dashed lines, variation of k_1 ±50%; dotted line, background (non-benzyl) absorbance.

For the experiments described here the absorption contributions due to benzyl, benzyl fragments, toluene, ethyl iodide, and ethylene were accounted for. Therefore, the measured fractional absorption (I/I_0) is expressed, via Beer's law, in terms of the contribution to the absorbance by these five absorbing species

$$I/I_0 = \exp(-\text{absorbance}) = \exp(-L\sum \sigma_i n_i)$$

where the sum is over the cross-section number density product of the following species: $C_6H_5CH_2$, C_7H_6, $C_6H_5CH_3$, C_2H_5I, and C_2H_4. In this formulation I is the transmitted laser intensity, I_0 is the reference beam intensity, σ_i [cm^2 molecule^{-1}] is the absorption cross-section of the individual absorbing species, n_i [molecules cm^{-3}] is the number density of the species, and L is the absorption path length (diameter of the shock tube, 14.13 cm). Fortunately, the background (non-benzyl) absorbance due to toluene, benzyl fragments, ethyl iodide, and ethylene for a given experiment was relatively constant over the duration of the experiment used to determine the rate coefficient due to the use of large concentrations of toluene relative to those of ethyl iodide in the test gas mixtures.

The absorbance at 266 nm for two example experiments is shown in Figures 1 and 3. Prior to the passage of the incident shock wave, a very low level of absorbance (∼0.1% in Figure 1) was detected at the low initial pressure, P_1. The passing of the incident shock wave causes a schlieren spike in the

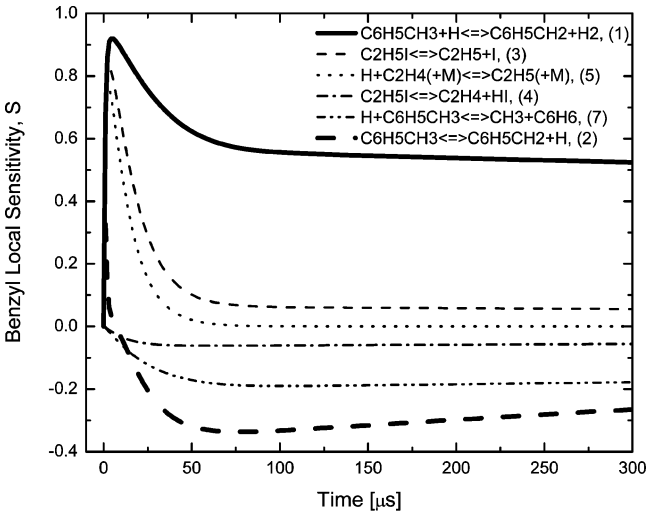

Figure 2. Local sensitivity for benzyl concentration for the conditions of the experiment given in Figure 1. $S = (dX_{benzyl}/dk_i)(k_i/X_{benzyl,local})$, where k_i is the rate coefficient for reaction i and $X_{benzyl,local}$ is the local benzyl ($C_6H_5CH_2$) mole fraction.

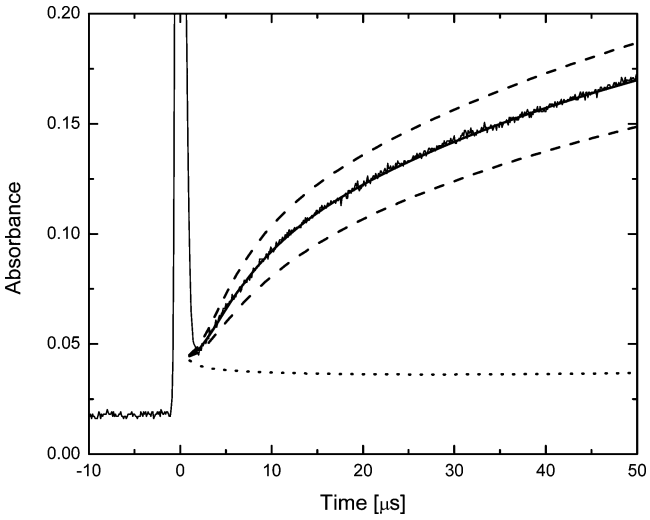

Figure 3. Example 266 nm absorbance. Reflected shock conditions: 1590 K, 1.66 bar, 50 ppm ethyl iodide/513 ppm toluene/argon. Solid line, fit to data by adjusting reaction 1 rate coefficient, k_1; dashed lines, variation of k_1 ±50%; dotted line, background (non-benzyl) absorbance.

absorbance trace (density deflection); the test gas is heated and compressed resulting in absorption due to toluene and ethyl iodide (~2% absorbance at $t \approx -70$ μs in Figure 1). The passage of the reflected shock wave causes another schlieren spike, and the toluene and ethyl iodide to absorb more strongly. After the passage of the reflected shock wave the ethyl iodide decomposes to yield an H-atom, and the benzyl absorbance grows primarily due to reaction 1 with influence from secondary chemistry, most notably the decomposition of toluene and the reverse, the recombination of H-atoms and benzyl to yield toluene (see the Modeling and Rate Coefficient Determination section for details).

As illustrated by the noise levels in Figures 1 and 3 an absorbance detection limit of approximately 0.1% ($\ln(I_0/I) = 0.001$) was provided by the laser absorption technique resulting in a peak signal-to-noise ratio of approximately 75 for the example shown in Figure 1 and a signal-to-noise ratio that ranges from 50 to 170 in the example shown in Figure 3. The benzyl detection limit ranged from 0.4 ppm at the lowest temperatures (~1260 K) to 0.6 ppm at the highest temperatures (~1660 K) of these experiments.

Modeling and Rate Coefficient Determination

Rate coefficient determinations for reaction 1 were determined by fitting the measured 266 nm absorbance by adjusting k_1 within a semidetailed mechanism (given in Table 1) and taking into account the contributions of the five absorbing species as described above. Note that reverse reactions were included (for the reactions written using the forward and backward arrow in Table 1) using the thermochemical data of Burcat and Ruscic[15] and the forward rate coefficients given in Table 1. For reactions written only in the forward direction (see reactions involving C_7H_6 and $C_6H_5CH_2CH_2C_6H_5$ in Table 1) adequate thermochemical data are not available for calculation of the reverse rate coefficients. In these cases the reverse reaction rate coefficients are directly included in the mechanism. The heats of formation from the Burcat and Ruscic thermochemical database used in modeling are given in Table 2.

The concentrations of ethyl iodide and toluene in the test gas mixtures were chosen to minimize the influence of secondary chemistry, while maintaining sufficient signal-to-noise such that the determined rate coefficients would have minimized uncertainty. Figures 1 and 3 illustrate two examples (one lower and one higher temperature example) of experimental absorbance and modeling fit made by adjusting k_1 within the Table 1 mechanism; the corresponding sensitivity calculations are shown in Figures 2 and 4. Note in Figures 1 and 3 that the background absorbance (dotted line) due to non-benzyl absorbers is almost constant over the course of the experiment as stated above. The measurements shown in Figures 1 and 3 are only given for test times for which we have absolute confidence in the measured benzyl profiles and for which sensitivity to secondary chemistry is minimized. At longer test times absorption due to interfering species not considered here (larger polycyclic aromatic hydrocarbons that eventually lead to soot formation) may confuse the interpretation of the absorption profiles. Additionally, interference due to secondary chemistry increases and the reaction mechanism used here is likely insufficient.

Following the passage of the reflected shock wave the ethyl iodide quickly undergoes a two-step thermal decomposition to produce H-atoms ($\tau < 5$ μs):

$$C_2H_5I \rightarrow C_2H_5 + I \quad (3)$$

$$C_2H_5 \rightarrow C_2H_4 + H \quad (5)$$

In addition a second, slower and non-H-atom producing, ethyl iodide decomposition channel was included in the kinetic mechanism:

$$C_2H_5I \rightarrow C_2H_4 + HI \quad (4)$$

The rate coefficients for reactions 3 and 4 were taken from Friedrichs et al.[16] who interpolated the results of Kumaran et al.[17] to provide rate expressions in the pressure range of our current experiments; the rate coefficient for reaction 5 was taken from Smith et al.[18] On the basis of the rates of Friedrichs et al. the H-atom yield from ethyl iodide decomposition following the reflected shock wave is 85−95% depending on the postshock experimental temperature. The ethyl iodide decomposition branching ratio used in the kinetic modeling slightly influences the determination of the rate coefficient for reaction 1 as indicated by the sensitivity analysis illustrated in Figures 2 and 4; for example if a 100% H-atom yield was used in the kinetic modeling instead of the branching ratio given above the k_1 determinations would decrease by approximately 7%. The

TABLE 1: Reaction Mechanism Used in Modeling Experimental Absorbance Traces, Rate Coefficients in the Form $k = AT^b \exp(-E_a/RT)$ where *A* has Units of cm, mol, and s, *T* has Units of K, and E_a Has Units of cal/mol

	reaction	*A*	b	E_a	ref
(1)	$C_6H_5CH_3 + H \leftrightarrow C_6H_5CH_2 + H_2$	6.47×10^0	3.98	3384	this study
(2)	$C_6H_5CH_3 \leftrightarrow C_6H_5CH_2 + H$ (1.5 bar)	2.09×10^{15}	0	87507	14
(3)	$C_2H_5I \leftrightarrow C_2H_5 + I$	3.66×10^9	0	26650	16
(4)	$C_2H_5I \leftrightarrow C_2H_4 + HI$	2.21×10^7	0	18953	16
(5)	$H + C_2H_4 \leftrightarrow C_2H_5$, high-pressure limit	3.78×10^{11}	0.454	1820	18
	low-pressure limit	4.20×10^{41}	−7.620	6970	
	Troe parameters	$a = 0.9753$			
		$b = 210.0$			
		$c = 984.0$			
		$d = 4374.0$			
(6)	$C_6H_5CH_2 \rightarrow C_7H_6 + H$	8.20×10^{14}	0	80670	13
(7)	$C_6H_5CH_3 + H \leftrightarrow C_6H_6 + CH_3$	5.78×10^{13}	0	8090	11
(8)	$C_6H_5CH_3 \leftrightarrow C_6H_5 + CH_3$ (1.5 bar)	2.66×10^{16}	0	97880	14
(9)	$C_7H_6 + H \rightarrow C_6H_5CH_2$	1.00×10^{14}	0	0	23
(10)	$C_6H_5 + H \leftrightarrow C_6H_6$	7.80×10^{13}	0	0	11
(11)	$C_6H_5 \leftrightarrow o\text{-}C_6H_4 + H$	8.00×10^{41}	−7.72	92210	24
(12)	$CH_3 + C_6H_5CH_3 \leftrightarrow C_6H_5CH_2 + CH_4$	3.16×10^{12}	0	0	25
(13)	$C_6H_5 + C_6H_5CH_3 \leftrightarrow C_6H_6 + C_6H_5CH_2$	7.94×10^{13}	0	11940	26
(14)	$C_6H_5CH_2 + C_6H_5CH_2 \rightarrow C_6H_5CH_2CH_2C_6H_5$	5.01×10^{12}	0	454	27
(15)	$C_6H_5CH_2CH_2C_6H_5 \rightarrow C_6H_5CH_2 + C_6H_5CH_2$	7.94×10^{14}	0	59751	27
(16)	$C_6H_5CH_2CH_2C_6H_5 \rightarrow C_6H_5CH_2CHC_6H_5 + H$	1.00×10^{16}	0	83660	28
(17)	$C_6H_5CH_2CH_2C_6H_5 + H \rightarrow C_6H_5CH_2CHC_6H_5 + H_2$	3.16×10^{12}	0	0	29
(18)	$C_6H_5CH_2CHC_6H_5 \rightarrow C_6H_5CHCHC_6H_5 + H$	7.94×10^{15}	0	51864	29

TABLE 2: Heats of Formation at 298 K (kcal/mol) Used in Modeling Experimental Absorbance Traces, from ref 15

species	$\Delta_f H^0_{298}$ [kcal/mol]
$C_6H_5CH_3$	11.99
$C_6H_5CH_2$	49.7
C_6H_6	19.81
C_6H_5	81.2
$o\text{-}C_6H_4$	26.3
C_2H_5I	−1.68
C_2H_5	28.36
C_2H_4	12.5
CH_4	17.83
CH_3	35.03
H_2	0
H	52.10
HI	6.30
I	25.52

uncertainties in k_3 and k_4 were taken into account in the uncertainty analysis for reaction 1.

Following ethyl iodide decomposition, the H-atoms react with the excess toluene present in the gas mixture to produce benzyl and molecular hydrogen. At temperatures below that which allow for the thermal decomposition of toluene (the example shown in Figure 1), the benzyl concentration grows due to reaction 1 and reaches a plateau which is maintained by a balance between reaction 1 and H-atom recombination with benzyl to yield toluene:

$$C_6H_5CH_3 + H \rightarrow C_6H_5CH_2 + H_2 \qquad (1)$$

$$C_6H_5CH_2 + H \rightarrow C_6H_5CH_3 \qquad (-2)$$

In the example illustrated in Figures 1 and 2, reaction 2 proceeds globally in the reverse direction throughout the experimental duration due to the experimental temperature which is too low to cause significant toluene dissociation and the large concentrations of H-atoms and benzyl. The rate coefficient for toluene dissociation, reaction 2, has been well characterized (uncertainty of ±35%) in the same facility used here at a pressure of 1.5 bar.[14] Therefore, we used the previous measurement of the forward rate k_2 and the well-known thermochemistry for toluene, benzyl, and H-atoms to calculate the reverse rate, k_{-2}. The thermochemical data of Burcat and Ruscic[15] was used with the following heats of formation for the three species involved in reaction 2: $\Delta_f H^0_{298}$(toluene) = 11.99 kcal/mol, $\Delta_f H^0_{298}$(benzyl) = 49.7 kcal/mol, and $\Delta_f H^0_{298}$(H) = 52.10 kcal/mol. The only reaction other than reactions 1 and 2 which shows sensitivity of note in Figure 2 is the dissociation of ethyl iodide which has been well characterized in multiple experiments.[17,19,20] The uncertainty in the rate coefficients for all secondary chemistry was taken into account in the estimation of the uncertainty in k_1 given below.

At temperatures high enough to cause the toluene in the test gas mixture to dissociate, the absorbance temporal behavior is somewhat different (see Figure 3) than the lower temperature example. Following the passage of the reflected shock wave the absorbance grows in a fashion similar to the lower temperature experiment in Figure 1. However, the absorbance never reaches a plateau; rather, the growth rate slows as function of

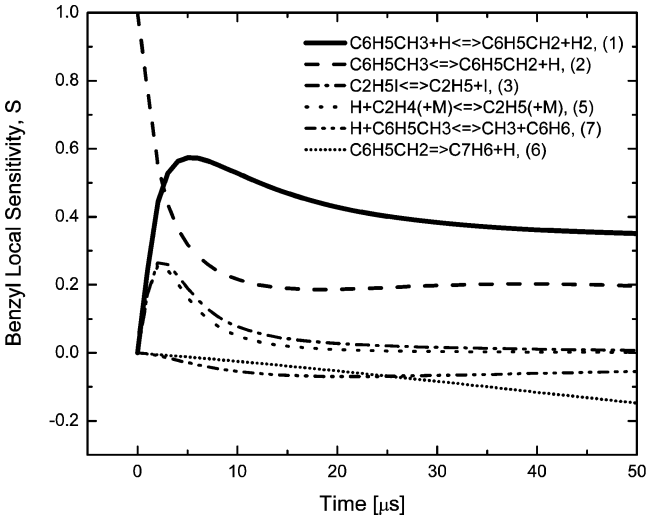

Figure 4. Local sensitivity for benzyl concentration for the conditions of the experiment given in Figure 3. $S = (dX_{benzyl}/dk_i)(k_i/X_{benzyl,local})$, where k_i is the rate coefficient for reaction *i* and $X_{benzyl,local}$ is the local benzyl ($C_6H_5CH_2$) mole fraction.

TABLE 3: Summary of Experimental Results

mixture	temp [K]	pressure [bar]	k_1 [cm^3 mol^{-1} s^{-1}]
50 ppm ethyl iodide/	1348	1.78	5.0×10^{12}
513 ppm toluene/argon	1356	1.85	5.2×10^{12}
	1379	1.77	5.8×10^{12}
	1437	1.73	7.5×10^{12}
	1479	1.72	8.7×10^{12}
	1526	1.73	1.0×10^{13}
	1590	1.66	1.2×10^{13}
	1650	1.57	1.4×10^{13}
30 ppm ethyl iodide/	1256	1.73	3.3×10^{12}
506 ppm toluene/argon	1258	1.86	3.7×10^{12}
	1313	1.87	4.4×10^{12}
	1363	1.78	5.5×10^{12}
	1369	1.90	5.2×10^{12}
	1445	1.78	7.5×10^{12}
	1511	1.72	9.4×10^{12}
	1601	1.67	1.3×10^{13}
	1667	1.67	1.4×10^{13}

time. At the higher temperature (1590 K) of this example the rate of toluene dissociation is significant, and the concentrations are such that globally reaction 2 proceeds in the forward direction

$$C_6H_5CH_3 \rightarrow C_6H_5CH_2 + H \quad (2)$$

Reaction 2 is the only secondary reaction that shows significant sensitivity at times longer than 10 μs as indicated by the small local sensitivity coefficients of the other reactions in Figure 4. This is true for all but the highest temperature experiments where benzyl decomposition

$$C_6H_5CH_2 \rightarrow C_7H_6 + H \quad (6)$$

shows increasing sensitivity. The rate coefficient for benzyl decomposition k_6 is greater than that for toluene decomposition k_2 over the entire temperature range of these experiments ($k_6/k_2 = 3.9$ at 1500 K). However, in the high-temperature example (Figures 3 and 4) the sensitivity coefficient for reaction 6 is smaller than the sensitivity coefficient for reaction 2 because the relative concentration of toluene to benzyl is large over the test time of these experiments used for k_1 determination ($[\text{toluene}]/[\text{benzyl}]_{\text{minimum}} = 6.4$ at 50 μs in the Figure 3 example). We have also previously measured k_6 with relatively small estimated uncertainty (±25%).[13]

Other reactions that show small or negligible sensitivity but are contained in the reaction mechanism are the reaction of H-atoms with toluene to yield benzene and methyl

$$C_6H_5CH_3 + H \rightarrow C_6H_6 + CH_3 \quad (7)$$

which is in direct competition with the title reaction and the toluene decomposition reaction producing phenyl and methyl

$$C_6H_5CH_3 \rightarrow C_6H_5 + CH_3 \quad (8)$$

Reactions 7 and 8 show negligible sensitivity because they are both slow relative to respective competing reactions 1 and 2 ($k_1/k_7 = 2.8$ and $k_2/k_8 = 2$ at 1600 K) and because k_1 was determined under conditions and time scales resulting in low conversion of toluene to products. Reaction 8 only serves to slightly reduce the toluene concentration and has negligible influence on the measured benzyl absorbance. Additionally, we have previously measured k_8 with an estimated uncertainty of ±35%.[14] Reaction 7 shows slightly greater although small sensitivity (see Figures 2 and 4) because it removes an H-atom that would otherwise produce a benzyl radical via reaction 1.

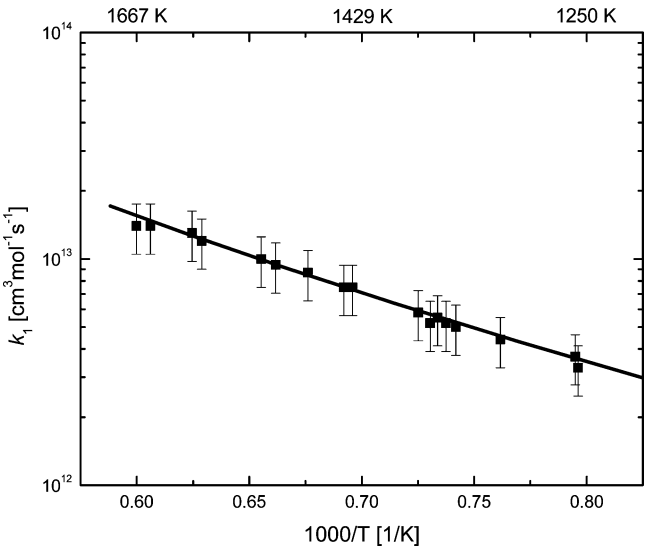

Figure 5. Rate coefficient results for reaction 1: filled squares with error bars, current experimental results; solid line, current three-parameter rate coefficient expression.

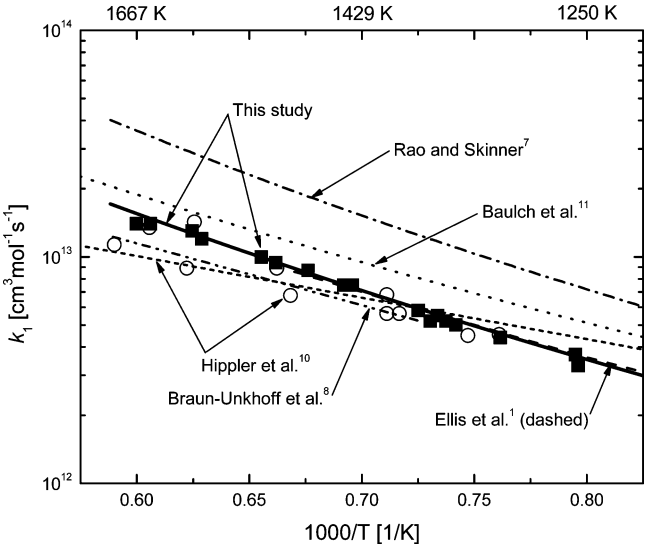

Figure 6. High-temperature reaction 1 rate coefficient comparison: filled squares, current experimental results; solid line, current three-parameter rate coefficient expression; dashed line, Ellis et al. extrapolation from 773 K measurement (obscured by current rate recommendation); open circles, Hippler et al. (ref 10) data; short-dashed line, Hippler et al.; dot-dashed line, Rao and Skinner (ref 7); dot-dot-dashed line, Braun-Unkhoff et al. (ref 8); dotted line, Baulch et al. (ref 11) survey recommendation.

The rate coefficient results of the current study are given in Table 3 and shown in Figure 5, with error bars representing an uncertainty estimate, and again in Figures 6 and 7 with comparison to previous studies. We estimate the uncertainty in the current results for k_1 to be ±25% with a 2σ probability. This uncertainty estimate is based on root-sum-squared (RSS) calculation taking into account uncertainty in temperature, pressure, initial mixture concentrations, secondary chemistry, absorption cross-sections, and fitting the data to computed profiles (uncertainty due to absorbance signal-to-noise). The largest source of uncertainty in the reaction 1 rate coefficient determinations comes from uncertainty in secondary chemistry and the benzyl absorption cross-section.

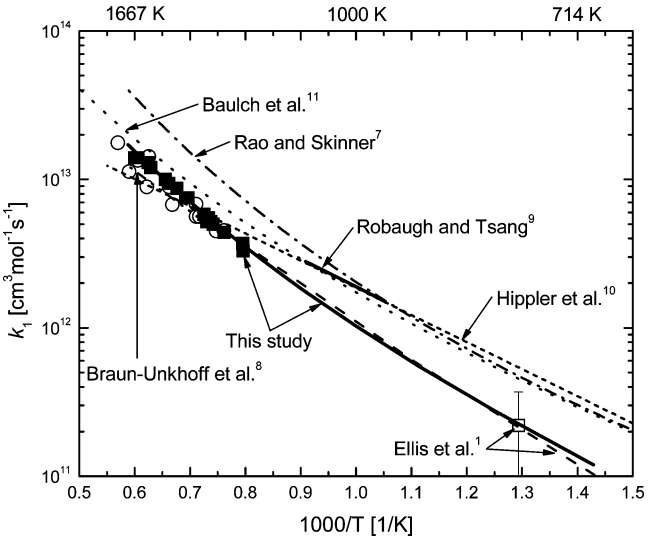

Figure 7. Reaction 1 rate coefficient comparison (larger temperature range): filled squares, current experimental results; solid line, current three-parameter rate coefficient expression; open square, Ellis et al. data point; dashed line, Ellis et al. extrapolation from 773 K measurement; open circles, Hippler et al. (ref 10) data; short-dashed line, Hippler et al.; dot-dashed line, Rao and Skinner (ref 7); solid line, Robaugh and Tsang (ref 9); dot-dot-dashed line, Braun-Unkhoff et al. (ref 8); dotted line, Baulch et al. (ref 11) survey recommendation.

The current data when fit using a simple two-parameter Arrhenius expression yields the following rate expression over the temperature range of the current experiments:

$$k_1(T) = 1.33 \times 10^{15} \exp(-14880\ [\text{cal/mol}]/RT)\ [\text{cm}^3\ \text{mol}^{-1}\ \text{s}^{-1}]$$

The measured activation energy is in agreement with several previous studies (local activation energies at 1500 K from previous studies are 16 730 cal/mol given by Rao and Skinner,[7] 13 370 cal/mol given by Baulch et al.,[11] 12 500 cal/mol given by Braun-Unkhoff et al.,[8] and 8370 cal/mol given by Hippler et al.[10]; see Figure 6) and is reasonable when compared to those of other H-atom abstraction reactions including $CH_4 + H \rightarrow CH_3 + H_2$ and $C_2H_4 + H \rightarrow C_2H_3 + H_2$.[21,22] However, the A-factor that results from the simple two-parameter fit is in excess of the collision limit. It is expected that reaction 1 should exhibit positive preexponential temperature dependence; therefore, a three-parameter fit is required to adequately represent the rate coefficient over a broad temperature range. Previous authors have also given rates for reaction 1 with positive preexponential temperature dependence.[1,7,11] We chose to fit a rate coefficient expression using both the current experimental results and the measurement of Ellis et al. at 773 K. As shown in Figure 7, the current data when extrapolated to lower temperatures agree very well with the result of the Ellis et al.[1] experiment (773 K). The rate coefficient expression that results from the combined fit of the current data and the measurement of Ellis et al. can be expressed as

$$k_1(T) = 6.47T^{3.98} \exp(-3384\ [\text{cal/mol}]/RT)\ [\text{cm}^3\ \text{mol}^{-1}\ \text{s}^{-1}]$$

where the temperature is in K and the rms experimental scatter in the data about the fit is ±4.4%. This rate coefficient expression can safely be used from 700 to 1800 K; however, the quoted uncertainty (±25%) can only be assumed in the range of the current experimental data. The very small rms experimental scatter is due to the high-absorbance signal-to-noise ratio provided by the spectrally intense laser source and the shot-to-shot consistency of the shock tube UV laser absorption experimental technique.

Discussion

A comparison of the current rate coefficient determinations with those of previous high-temperature experimental studies,[6−10] extrapolations of those experimental studies to lower temperatures, and the IUPAC recommendation of Baulch et al.[11] are shown in Figures 6 and 7. The current rate determinations are in fair agreement with the previous high-temperature shock tube UV benzyl absorption measurements of Hippler et al.;[10] however, the scatter in the current data is significantly reduced in comparison to that of their previous data (see Figure 6). The current rate results are approximately 25% higher than the shock tube H-atom ARAS measurements of Braun-Unkhoff et al.[8] and approximately a factor of 2.5 lower than the D-atom and H-atom ARAS measurements of Rao and Skinner;[7] however, the results of Rao and Skinner show agreement with the current study for the activation energy. The results of Robaugh and Tsang[9] (950−1100 K) would seem to agree in magnitude with the current experimental results when extrapolated to higher temperatures. However, the activation energy of Robaugh and Tsang[9] is low when compared to the current data and their rate is approximately a factor of 2 higher at 1000 K when compared to the current rate expression that results from the combination of the current measurements and the measurement of Ellis et al.[1] The current data set when extrapolated to lower temperatures is in excellent agreement with the measurement at 773 K made by Ellis et al.[1] and therefore, as described above, we fit the rate coefficient expression using both the current data and the data point of Ellis et al. Additionally, the current data are in excellent agreement with the extrapolation to higher temperatures recommended by Ellis et al. which is based on extrapolation of their lower temperature data point to high temperature using the data of Hippler et al.[10]

The Baulch et al.[11] review recommendation (600−2500 K) is higher than the current rate measurement (see Figure 6) and the current rate expression (see Figure 7). The Baulch et al. review states that their recommendation is based on the data of refs 7−10. However, this statement is confusing in view of the disagreement in these studies as evident in Figures 6 and 7. It appears that the Baulch et al. recommendation is a compromise, or average, at high temperatures between the high Rao and Skinner measurements, the low Hippler et al. measurements (which are in fair agreement with the current study), and the lower Braun-Unkhoff et al. measurements. The Baulch et al. recommendation is consistent with the results of Robaugh and Tsang at lower temperatures (950−1100 K) and therefore is high in comparison to the rate expression given here. The recommendation made by Hippler et al.[10] over the larger temperature range (600−1800 K) was made by extrapolating their high-temperature data (1300−1700 K) to lower temperatures using the results of Robaugh and Tsang[9] (950−1100 K) and an unpublished lower temperature study by Ravishankara and Nicovich. The Hippler et al. recommendation, like the Baulch et al. recommendation, is also in disagreement with the current rate expression given at lower temperatures ($T < 1200$ K).

Conclusions

The reaction of toluene with H-atoms to produce benzyl and molecular hydrogen has been studied at temperatures ranging from 1256 to 1667 K at total pressures around 1.7 bar using

shock wave heating and UV laser absorption of benzyl at 266 nm. The 266 nm benzyl absorption traces allowed determination of the rate coefficient for reaction 1. The high levels of signal-to-noise provided by the laser absorption technique allowed for the determination of k_1 with an uncertainty of ±25%. The rate coefficient measurements are in fair agreement with the previous measurements of Hippler et al.;[10] however, the scatter and uncertainty in the current data is reduced. The rate expression given here is based on combination of the current data with the 773 K measurement of Ellis et al.[1] and is in agreement with an estimated extrapolation to higher temperatures made by Ellis et al.[1]

Acknowledgment. This work was performed at Stanford University and supported by the U.S. Department of Energy, Chemical Sciences Division, Office of Basic Energy Sciences, with Dr. Frank Tully as contract monitor.

References and Notes

(1) Ellis, C.; Scott, M. S.; Walker, R. W. *Combust. Flame* **2003**, *132*, 291.
(2) Hippler, H.; Reihs, C.; Troe, J. *Proc. Combust. Inst.* **1990**, *23*, 37.
(3) Pitz, W. J.; Seiser, R.; Bozzelli, J. W.; Da Costa, I.; Fournet, R.; Billaud, F.; Battin-Leclerc, F.; Seshadri, K.; Westbrook, C. K. In *Proceedings of the 2nd Joint Meeting of the U.S. Sections of the Combustion Institute*; 2001.
(4) Bounaceur, R.; Da Costa, I.; Fournet, R.; Billaud, F.; Battin-Leclerc, F. *Int. J. Chem. Kinet.* **2005**, *37*, 25.
(5) Dagaut, P.; Pengloan, G.; Ristori, A. *Phys. Chem. Chem. Phys.* **2002**, *4*, 1846.
(6) Rao, V. S.; Skinner, G. B. *J. Phys. Chem.* **1984**, *88*, 4362.
(7) Rao, V. S.; Skinner, G. B. *J. Phys. Chem.* **1989**, *93*, 1864.
(8) Braun-Unkhoff, M.; Frank, P.; Just, Th. *Proc. Combust. Inst.* **1989**, *22*, 1053.
(9) Robaugh, D.; Tsang, W. *J. Phys. Chem.* **1986**, *90*, 4159.
(10) Hippler, H.; Reihs, C.; Troe, J. *Z. Phys. Chem. (Neue Folge)* **1990**, *167*, 1.
(11) Baulch, D. L.; Bowman, C. T.; Cobos, C. J.; Cox, R. A.; Just, Th.; Kerr, J. A.; Pilling, M. J.; Stocker, D.; Troe, J.; Tsang, W.; Walker, R. W.; Warnatz, J. *J. Phys. Chem. Ref. Data* **2005**, *34*, 757.
(12) Oehlschlaeger, M. A.; Davidson, D. F.; Hanson, R. K. *J. Phys. Chem. A* **2004**, *108*, 4247.
(13) Oehlschlaeger, M. A.; Davidson, D. F.; Hanson, R. K. *J. Phys. Chem. A* **2006**, *110*, 6649.
(14) Oehlschlaeger, M. A.; Davidson, D. F.; Hanson, R. K. *Proc. Combust. Inst.*, in press.
(15) Burcat, A.; Ruscic, B. Ideal Gas Thermochemical Database with Updates from Active Thermochemical Tables. ftp://ftp.technion.ac.il/pub/supported/aetdd/thermodynamics (April 2006), mirrored at http://garfield.chem.elte.hu/burcat/burcat.html (April 2006).
(16) Friedrichs, G.; Davidson, D. F.; Hanson, R. K. *Int. J. Chem. Kinet.* **2002**, *34*, 374.
(17) Kumaran, S. S.; Su, M.-C.; Lim, K.; Michael, J. V. *Proc. Combust. Inst.* **1996**, *26*, 605.
(18) Smith, G. P.; Golden, D. M.; Frenklach, M.; Moriarty, N. W.; Eiteneer, B.; Goldenberg, M.; Bowman, C. T.; Hanson, R. K.; Song, S.; Gardiner, W. C., Jr.; Lissianski, V. V.; Qin, Z. GRI-Mech 3.0. http://www.me.berkeley.edu/gri_mech/ (2003).
(19) Mertens, J. D.; Wooldridge, M. S.; Hanson, R. K. In *Proceedings of the U.S. Eastern States Section of the Combustion Institute*; 1994.
(20) Wintergerst, K.; Frank, P. *Proceedings of the 19th Symposium (International) on Shock Waves and Tubes*; Springer-Verlag: New York, 1994; p 78.
(21) Knyazev, V. D.; Bencsura, A.; Stoliarov, S. I.; Slagle, I. R. *J. Phys. Chem.* **1996**, *100*, 11346.
(22) Sutherland, J. W.; Su, M.-C.; Michael, J. V. *Int. J. Chem. Kinet.* **2001**, *33*, 669.
(23) Eng, R. A.; Gebert, A.; Goos, E.; Hippler, H.; Kachiani, C. *Phys. Chem. Chem. Phys.* **2002**, *4*, 3989.
(24) Madden, L. K.; Moskaleva, L. V.; Kristyan, S.; Lin, M. C. *J. Phys. Chem. A* **1997**, *101*, 6790.
(25) Litzinger, T. A.; Brezinsky, K.; Glassman, I. *Combust. Flame* **1986**, *63*, 251.
(26) Heckmann, E.; Hippler, H.; Troe, J. *Proc. Combust. Inst.* **1996**, *26*, 543.
(27) Hippler, H.; Troe, J. *J. Phys. Chem.* **1990**, *94*, 3803.
(28) Hippler, H.; Reihs, C.; Troe, J. *Proc. Combust. Inst.* **1990**, *23*, 37.
(29) Brouwer, L. D.; Müller-Markgraf, W.; Troe, J. *J. Phys. Chem.* **1988**, *92*, 4905.